

## Discrepancy of room temperature ferromagnetism in Mo-doped $\text{In}_2\text{O}_3$

O M LEMINE<sup>1,\*</sup>, M BOUODINA<sup>2,3</sup>, E K HLIL<sup>4</sup>, A AL-SAIE<sup>2,3</sup>, A JAAFAR<sup>2</sup>,  
A ALYAMANF<sup>5</sup> and B OULADDIAF<sup>6</sup>

<sup>1</sup>Physics Department, College of Science, Al-Imam Mohammad Ibn Saud Islamic University (IMSIU), Riyadh, Saudi Arabia

<sup>2</sup>Nanotechnology Centre, University of Bahrain, Sakhir, Kingdom of Bahrain

<sup>3</sup>Department of Physics, College of Science, University of Bahrain, Sakhir, Kingdom of Bahrain

<sup>4</sup>Institut Néel, CNRS - Université J. Fourier, BP 166, 38042 Grenoble, France

<sup>5</sup>National Nanotechnology Research Centre, KACST, Riyadh, Saudi Arabia

<sup>6</sup>Institut Laue Langevin, Grenoble, France

MS received 18 November 2011; revised 17 March 2012

**Abstract.** Molybdenum-doped indium oxide nanopowders were synthesized via mechanical alloying with subsequent annealing at a relatively low temperature of 600 °C. The morphologies and crystal structures of the synthesized nanopowders were examined by using scanning electron microscopy (SEM) and X-ray diffraction patterns. X-ray diffraction pattern of the milled mixture shows the presence of both  $\text{In}_2\text{O}_3$  phase and Mo element. The presence of broad peaks in the pattern confirms that the synthesized powders are nanosized. The X-ray diffraction of annealed samples at 600 °C shows the absence of Mo peaks revealing that the Mo was incorporated into the crystal lattices of  $\text{In}_2\text{O}_3$ . Interestingly, it was observed that the diffraction peaks were still broad in the annealed samples indicating the single phase at the nanoscale. From the XRD pattern, the calculated crystallite sizes were in the range of 12–18 nm. Magnetic properties of the synthesized Mo-doped  $\text{In}_2\text{O}_3$  nanopowders were examined and it was found that the obtained nanopowders possess diamagnetic properties.

**Keywords.** Nanopowder; transparent conducting; diamagnetic.

### 1. Introduction

Transparent conducting oxides (TCOs) exhibit exceptional combined properties, high electrical conductivity and high optical transparency; therefore, they offer a wide range of technological applications including thin film photovoltaic, smart windows, organic light emitting diodes, flat-panel displays, etc (Ginley and Bright 2000).

Among various TCOs, indium tin oxides (ITO) have special place due to their versatile properties and applications. Indium tin oxides (ITO), where  $\text{In}_2\text{O}_3$  is doped with some amount of Sn in the range of 5–10 wt%, have been investigated and used as transparent conducting panels for electromagnetic shielding or anti-static applications (Ginley and Bright 2000).

Recently,  $\text{In}_2\text{O}_3$  has been doped with molybdenum, generating a new family of transparent conductors known as IMO (Meng *et al* 2001; Warmsingh *et al* 2004; Miao *et al* 2006). In these previous reported works about TCOs, the investigated compositions were mainly thin films prepared by various techniques. Moreover, according to the existing reports, ITO nano powders have been prepared by solvothermal procedure (Lee and Choi 2005; Jeon and Kang 2008), co-precipitation (Li *et al* 2006), emulsion (Sujatha Devi *et al*

2002) and sol–gel method (Han *et al* 2007; Yang *et al* 2009), evaporation (Shigesato *et al* 1993), spray pyrolysis (Beaurain *et al* 2008) and screen printing (Bessais *et al* 1993).

Mechanical alloying as a solid state process is a powerful technique for chemical alloying and microstructure modifications and offers many possibilities in the preparation of new materials at the nano-scale with improved properties including non-equilibrium phases (supersaturated solid solutions, amorphous phases) (Suryanarayana 2001). In a previous work, the authors have investigated  $\text{In}_2\text{O}_3 + 10 \text{ wt\% SnO}$  mixture, where a complete dissolution of SnO into  $\text{In}_2\text{O}_3$  lattice to form a pure  $(\text{In}, \text{Sn})_2\text{O}_3$  phase has been obtained after milling without applying subsequent annealing (Al-Saie *et al* 2009). It is worthy also to report that, doping  $\text{In}_2\text{O}_3$  with Mo leads to the formation of magnetically mediated transparent conductor (Medvedeva 2006). Based on first-principles band structure calculations (Medvedeva 2006), it is found that the change in optical absorption and electrical conductivity of doping  $\text{In}_2\text{O}_3$  with a transition metal, is not only due to the number of carriers brought by the doping element such as the case of Sn, but also due to the magnetic interactions. More recently, Park *et al* (2009) reported that  $\text{In}_2\text{O}_3$  film is ferromagnetic at room temperature while doped with Mo results in an enhancement of ferromagnetism. Therefore, this present work will be devoted to the synthesis and the investigation of the magnetic properties of  $\text{In}_2\text{O}_3$  powder doped with 10 at% of Mo.

\*Author for correspondence (leminej@yahoo.com)

The purpose of this study is (i) to produce Mo-doped  $\text{In}_2\text{O}_3$  nanopowders with high concentration of Mo (10 wt%) and (ii) to produce a diluted magnetic material for electronic and magnetic devices while maintaining the transparency and electrical conductivity of the parent material ( $\text{In}_2\text{O}_3$ ). To our knowledge, no paper in the literature has reported the synthesis of  $\text{In}_2\text{O}_3$  nanopowder doped with Mo. The only reported work has been devoted to thin films (Park *et al* 2009).

## 2. Experimental

All chemicals were used as received.  $\text{In}_2\text{O}_3$  (99.7%) and pure molybdenum metal (99.7%) powders were supplied by Fluka AG. The milling was carried out using a planetary mill premium line (P7). Both balls and bowl were made of zirconium oxide ( $\text{ZrO}_2$ ) to avoid any contamination. The milling was carried out under air with a speed of 300 rpm for 20 h and a balls/powder ratio of 20.

Powder X-ray diffraction (XRD) measurements were carried out using Phillips 1710 diffractometer equipped with  $\text{CuK}\alpha$  radiation ( $\lambda = 1.5418 \text{ \AA}$ ). The crystallites size (CS) and the microstrains (MS) were estimated using peak profile analysis with a software provided with the diffractometer, where the full width at half maximum (FWHM) is determined, then used for the calculation by introducing a standard value for instrument contribution to the peak broadening. Microstructure and chemical analysis were studied using Nova NanoLab field emission scanning microscope equipped with an electron dispersive X-ray spectrometer (EDS). Magnetic-hysteresis loop measurements were carried out at room temperature using PMC MicroMag 3900 model vibrating sample magnetometer (VSM) equipped with 1 Tesla magnet.

## 3. Results and discussion

Figure 1 shows evolution of X-ray diffraction (XRD) of the milled  $\text{In}_2\text{O}_3 + 10 \text{ wt\% Mo}$  mixture and after annealing at  $600 \text{ }^\circ\text{C}$ . Both  $\text{In}_2\text{O}_3$  and Mo diffraction peaks remain after milling and no additional peaks have been observed. This indicates that no solid state reaction occurred and no impurity has been formed. It is clear that after 20 h of milling, the main diffraction peaks of  $\text{In}_2\text{O}_3$  phase become very broader and their intensity decreases drastically compared to as-received  $\text{In}_2\text{O}_3$  powder. This is mainly due to particle's size reduction and accumulation of microstrains during mechanical milling. It is noticed that Mo peaks are less broader compared to  $\text{In}_2\text{O}_3$  peaks, probably due to the mechanical properties, Mo metal is harder.

To investigate the effect of annealing on the structure stability and microstructure parameters (crystallite size and microstrains), the milled powder was annealed at  $600 \text{ }^\circ\text{C}$  for a period of 1 h. It is important to note that after annealing, Mo peaks completely disappear, suggesting a complete

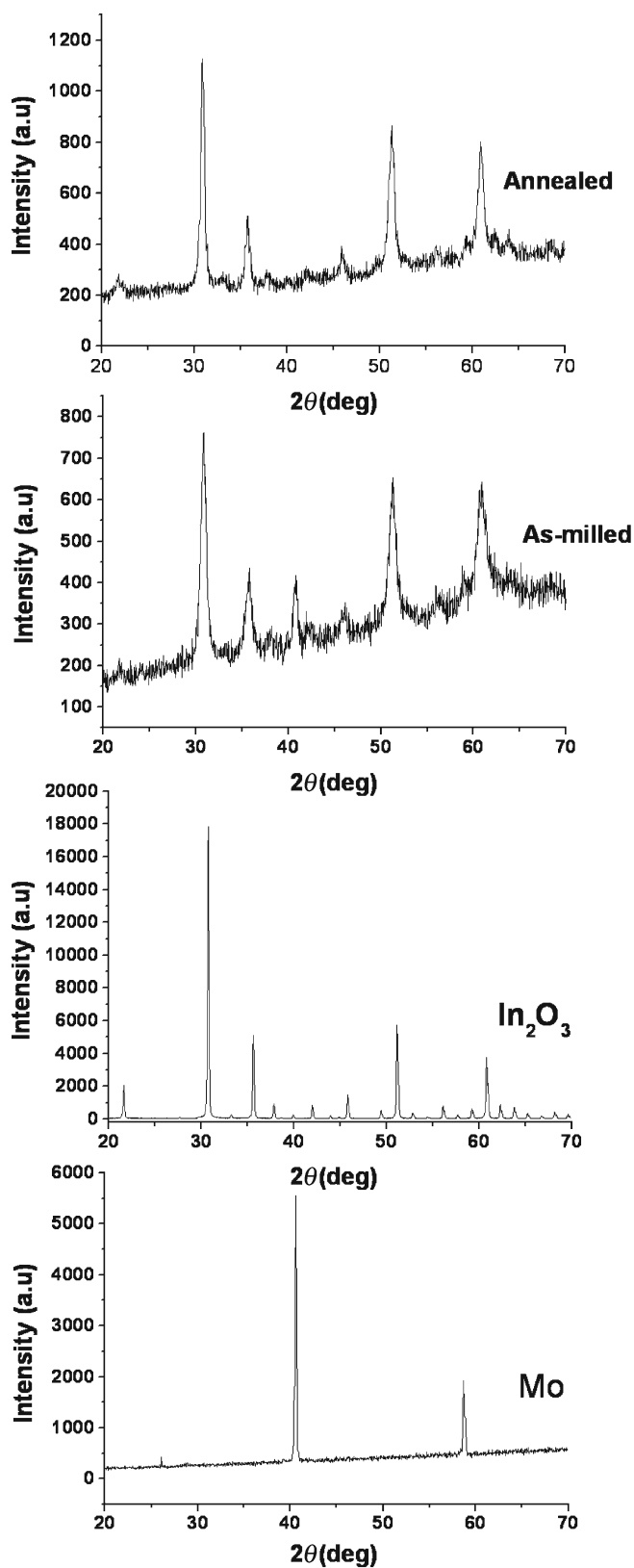


**Figure 1.** XRD patterns of as-received  $\text{In}_2\text{O}_3$ , Mo metal, Mo- $\text{In}_2\text{O}_3$  milled mixture and annealed mixture at  $600 \text{ }^\circ\text{C}$ .

dissolution of Mo into  $\text{In}_2\text{O}_3$  host matrix, without altering its crystal structure. As it can be clearly noticed, the position of the main peak of  $\text{In}_2\text{O}_3$  phase (222), changes its

**Table 1.** Microstructural parameters, i.e. crystallite size (CS) estimated from X-ray diffraction analysis and magnetization at maximum field (10 kOe).

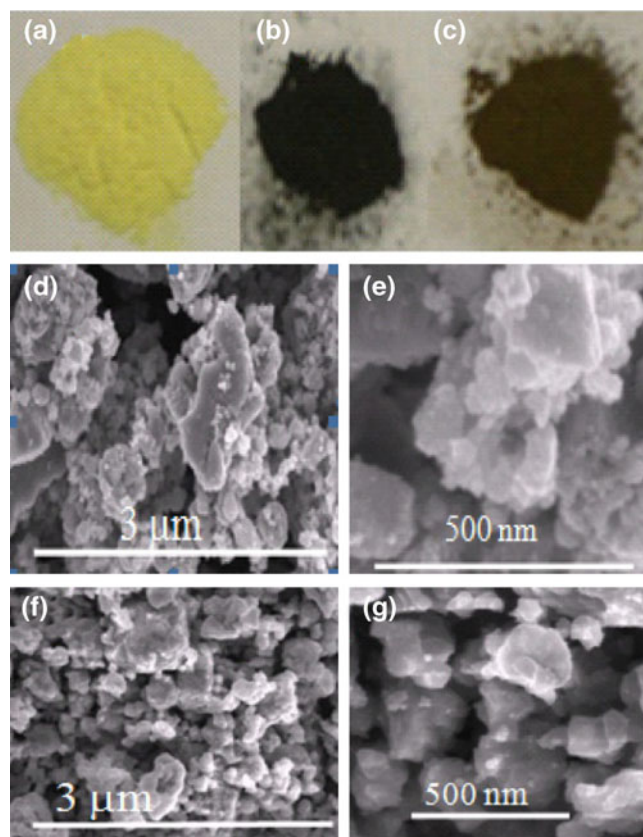
Sample	CS (nm)	Magnetization ( $\mu$ emu/g)
$\text{In}_2\text{O}_3$ as received	–	1.8
Mo metal	–	0.01
Milled Mo– $\text{In}_2\text{O}_3$ mixture	12	20.1
Annealed milled mixture	18	16.1

position after annealing associated to the change of the lattice parameters due to substitution. The peak position has shifted to higher angles, indicating a volume contraction of the lattice, which confirms the substitution of Mo into In ionic sites, in accordance with ionic radii reduction:  $r(\text{In}^{3+}$  in  $\text{In}_2\text{O}_3$ ) = 0.92 Å and  $r(\text{Mo}^{6+})$  = 0.68 Å or  $r(\text{Mo}^{4+})$  = 0.65 Å (Smith and Hashemi 2006), in agreement with previous results reported by Meng *et al* (2001). Table 1 reports the structural parameters estimated from peak profile analysis. The microstructural parameters, i.e. the crystallites size and the microstrains, were estimated using peak profile analysis by a software provided with the diffractometer, where the full width at half maximum (FWHM) is determined, then used for the calculation by introducing a standard value for the instrument contribution to the peak broadening. The estimated crystallites size of the as-milled powder is the nanoscale, around 12 nm while, after annealing, it increases slightly up to 18 nm due to crystal growth.

It should also be noticed that the colour of the pellet has changed from yellow for as-received  $\text{In}_2\text{O}_3$  powder to black after milling and finally to grayish after annealing, a confirmation of the formation of  $(\text{In}, \text{Mo})_2\text{O}_3$  phase, (see figures 2(a–c)).

Scanning electron microscopy images are reported in figure 2. It is clear that after milling (figures 2(d) and (e)), both  $\text{In}_2\text{O}_3$  and Mo metal remain without any interaction with a decrease in particle size.  $\text{In}_2\text{O}_3$  particles form agglomerates with particles size ranging in the nanometer scale while Mo particles are much larger, due to the fact that Mo is a harder metal, in good agreement with crystallites size estimated from X-ray diffraction peaks. After annealing (figures 2(f) and (g)), only bright with homogenous particle size distribution were observed, an indication that solid-state interaction occurred between  $\text{In}_2\text{O}_3$  and Mo to form a new pseudo-binary  $(\text{In}, \text{Mo})_2\text{O}_3$  phase.

Chemical analysis, reported in table 2, shows the presence of only In and Mo elements, which clearly indicates that no contamination has occurred during milling. It is important to note that the ratio In/Mo of the milled sample is a bit higher, i.e. 12.2 than the starting composition, i.e. 9, due to the fact that Mo particles may not be homogeneously distributed among the main phase,  $\text{In}_2\text{O}_3$ . After annealing, this ratio becomes 10.1, closer to the starting composition.

**Figure 2.** Photographs of powders of (a) as-received  $\text{In}_2\text{O}_3$ , (b) milled Mo– $\text{In}_2\text{O}_3$ , (c) milled mixture after annealing, SEM images of (d)  $\text{In}_2\text{O}_3$ –Mo as milled at lower magnification, (e)  $\text{In}_2\text{O}_3$ –Mo as milled at higher magnification, (f)  $\text{In}_2\text{O}_3$ –Mo as milled and annealed at 600 °C at lower magnification and (d)  $\text{In}_2\text{O}_3$ –Mo as milled and annealed at 600 °C at higher magnification.**Table 2.** Chemical analysis (at%) obtained by electron dispersive X-ray spectroscopy (EDS) analysis.

Sample	Milled Mo– $\text{In}_2\text{O}_3$	Annealed milled mixture
In	7.6	9.0
Mo	92.4	91.0
In/Mo ratio	12.2	10.1

Hysteresis loop measurements, shown in figure 3, have been carried out on Mo metal, of the as-received  $\text{In}_2\text{O}_3$ , as well as milled and annealed  $\text{In}_2\text{O}_3$ –Mo mixture. It is noticed that the parent compound  $\text{In}_2\text{O}_3$  is diamagnetic while Mo metal is paramagnetic. After doping with Mo, the dissolution of Mo atoms into  $\text{In}_2\text{O}_3$  crystal structure by occupying indium metal sites did not induce a strong magnetic contribution to the diamagnetic  $\text{In}_2\text{O}_3$  parent compound: the pseudo-binary compound  $(\text{In}, \text{Mo})_2\text{O}_3$  remains diamagnetic with a slight decrease of the absolute value of magnetization at the

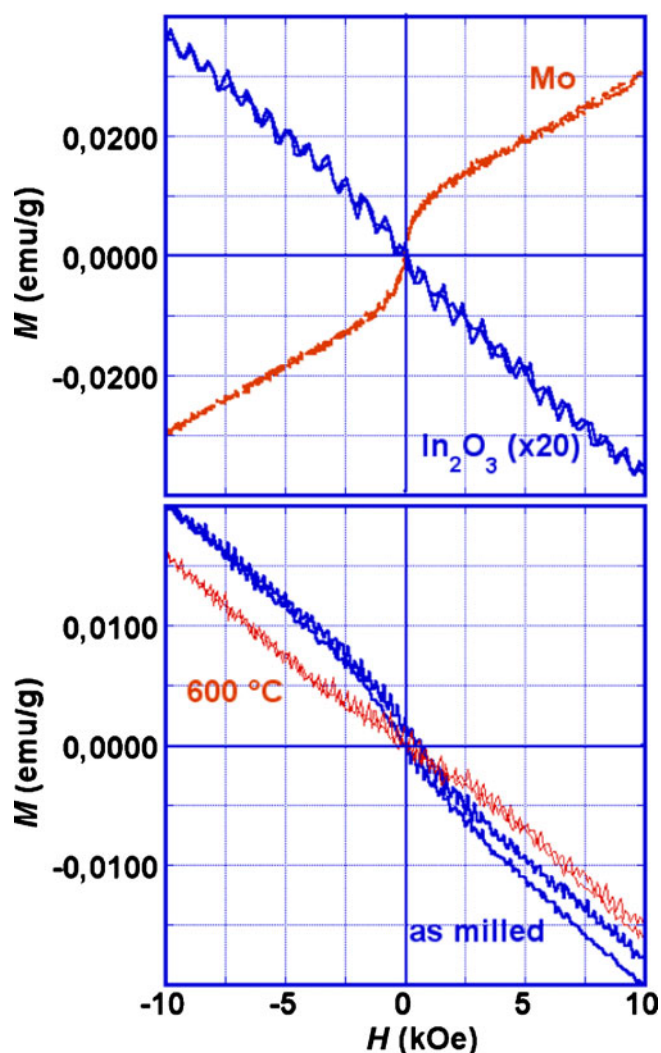


**Figure 3.** Hysteresis loop of as-received  $\text{In}_2\text{O}_3$ , Mo metal, Mo– $\text{In}_2\text{O}_3$  milled mixture and Mo– $\text{In}_2\text{O}_3$  milled mixture after annealing at 600 °C.

maximum field (10 kOe). This result is not in agreement with the most recent results reported by Park *et al* (2009). The authors prepared thick films of Mo-doped indium oxide on (100) MgO substrates at 450 °C using pulsed laser deposition (PLD) technique. It is found that an undoped  $\text{In}_2\text{O}_3$  is ferromagnetic at room temperature while doped with Mo metal enhances the ferromagnetism by increasing the saturation magnetization. The observed ferromagnetism in pure  $\text{In}_2\text{O}_3$  film is ascribed to the oxygen vacancies, whereas the enhancement of ferromagnetism in Mo-doped  $\text{In}_2\text{O}_3$  films is ascribed to the fact that Mo may occupy both indium sites. But assuming all Mo atoms occupy indium (1) sites gives an estimated saturation magnetization for the 5 wt% Mo film around 0.8 emu/cc, which is nearly an order of magnitude smaller than the value reported by the authors (Park *et al* 2009). The discrepancy between reported work on thick films and this study can be summarized as follows: (i) In the PLD method the synthesis route is oxygen free. Hence replacing

In ( $\text{In}^{3+}$ ) by Mo ( $\text{Mo}^{4+}$ ,  $\text{Mo}^{6+}$ ) automatically induces non-equilibrium charge distribution of the pseudo-binary compound  $\text{In}_{2-x}\text{Mo}_x\text{O}_3$ ; the extra positive charges brought by Mo will depend on the content  $x$  of Mo and its oxidation state, which results in extra oxygen vacancies therefore enhancing the ferromagnetism already observed in pure  $\text{In}_2\text{O}_3$  film; (ii) However, in this work, the milled  $\text{In}_2\text{O}_3$ –Mo mixture was annealed at 600 °C under air and after reaction, Mo dissolves into  $\text{In}_2\text{O}_3$  lattice by occupying In sites. Therefore and as stated before, this induces a non-equilibrium charge distribution which will be compensated by oxygen from air resulting in the formation of non-stoichiometric pseudo-binary compound  $\text{In}_{2-x}\text{Mo}_x\text{O}_{3+y}$ , where the value of  $y$  depends again on the content of Mo and its oxidation state. This oxygen deficiency may be the origin of the diamagnetic behaviour observed during magnetic measurements (see figure 3). This can be supported by a previous study on the effect of oxygen deficiency in the magnetic behaviour of the perovskite  $\text{RBaCuFeO}_{5+y}$  compounds (where  $R = \text{Y}$  or  $\text{Pr}$ ). The magnetic structure of these materials was determined by neutron diffraction experiments and gives an evidence that the introduction of extra oxygen destroys the magnetic ordering if  $R = \text{Pr}$ , i.e.  $\text{PrBaCuFeO}_{5+y}$  (Blackman and Trohidou 1997).

#### 4. Conclusions

In conclusion, nanocrystalline powder of Mo-doped  $\text{In}_2\text{O}_3$  phase was obtained by a simple combination of mechanical milling with subsequent annealing at low temperature of 600 °C for 1 h. It is very important to note that, till now, such high Mo doping concentration has not been reported in the literature. Magnetic measurements show a diamagnetic behaviour after doping in discrepancy with reported work on thick films. Further investigations are underway to understand such discrepancy between powder and thin films, including neutron diffraction analysis, band structure calculations and the synthesis of new compositions.

#### References

- Al-Saie A, Arekat S, Jaafer A and Bououdina M 2009 *Int. J. Nanopart.* **2** 507
- Beaurain A, Luxembourg D, Dufour C, Koncar V, Capoen B and Bouazaoui M 2008 *Thin Solid Films* **516** 4102
- Bessaïs B, Mliki N and Bennaceur R 1993 *Semicond. Sci. Technol.* **8** 116
- Blackman J A and Trohidou K N 1997 *J. Appl. Phys.* **81** 5293
- Ginley D S and Bright C 2000 *MRS Bull.* **25** 15
- Han Chi-Hwan, Han Sang-Do, Gwak Jihye and Khatkar S P 2007 *Mater. Lett.* **61** 1701
- Jeon Min-Kyu and Kang Misook 2008 *Mater. Lett.* **62** 676
- Lee Jin-Seok and Choi Sung-Churl 2005 *J. Eur. Ceram. Soc.* **25** 3307
- Li Shitao, Qiao Xueliang, Chen Jianguo, Wang Hongshui, Jia Fang and Qiu Xiaolin 2006 *J. Cryst. Growth* **289** 151

- Medvedeva J E 2006 *Phys. Rev. Lett.* **97** 086401
- Meng Yang, Yang Xi-Liang, Chen Hua-Xian, Shen Kie, Jiang Yi-Ming, Zhang Zhuang-Jian and Hua Zhong-Yi 2001 *Thin Solid Films* **394** 219
- Miao Wei-Na, Li Xi-Feng, Zhang Qun, Huang Li, Zhang Zhuang-Jian, Zhang Li and Yan Xue-Jian 2006 *Thin Solid Films* **500** 70
- Park Chang-Yup, Yoon Soon-Gil, Young-Hun and Shin Sung-Chul 2009 *Appl. Phys. Lett.* **95** 122502
- Shigesato Y, Paine D C and Hayens T E 1993 *Jpn J. Appl. Phys.* **32** L1352
- Smith W F and Hashemi J (eds) 2006 *Foundations of materials science and engineering* (Singapore: McGraw Hill International Edition) 4th ed.
- Sujatha Devi P, Chatterjee M and Ganguli D 2002 *Mater. Lett.* **55** 205
- Suryanarayana C 2001 *Prog. Mater. Sci.* **46** 1
- Warmingsingh C, Yoshida Y, Readey D W, Teplin C W, Perkins J D, Gedvilas P A, Keyes B M and Ginley D S 2004 *J. Appl. Phys.* **95** 3831
- Yang L L, He X D, He F and Sun Y 2009 *J. Alloys Compd* **470** 317